

PACS numbers: 61.72.Mm, 68.35.Ct, 68.37.Ps, 68.55.A-, 68.55.J-, 81.15.Cd, 81.15.Gh

Surface Morphology of $(\text{La}_{0.06}\text{Ga}_{0.94})_2\text{O}_3:\text{Eu}$ Thin Films

O. M. Bordun¹, B. O. Bordun¹, I. I. Medvid¹, M. V. Protsak¹,
K. L. Biliak¹, I. Yo. Kucharsky¹, D. M. Maksymchuk¹,
I. M. Kofliuk¹, and D. S. Leonov²

¹*Ivan Franko National University of Lviv,
50, Drahomanov Str.,
UA-79005 Lviv, Ukraine*

²*Technical Centre, N.A.S. of Ukraine,
13, Pokrovska Str.,
UA-04070 Kyiv, Ukraine*

Thin films of $(\text{La}_{0.06}\text{Ga}_{0.94})_2\text{O}_3:\text{Eu}$ are obtained by radio-frequency (RF) ion-plasma sputtering in an argon atmosphere on single-crystal NaCl and amorphous $\nu\text{-SiO}_2$ substrates. The study of the surface morphology of thin films by atomic force microscopy (AFM) shows that the average diameter of crystallites forming the film increases from 23 nm to 48 nm, when there is switching from NaCl to $\nu\text{-SiO}_2$ substrates. The heat treatment of films on $\nu\text{-SiO}_2$ substrates in an argon atmosphere leads to the increase in the average grain diameters to 68 nm and, accordingly, the root-mean-square roughness from 0.5 nm to 6.1 nm. The analysis of the distributions of crystallites by diameter and volume is carried out, and it is proposed that, in the process of RF sputtering, secondary grains grow, and in the process of high-temperature heat treatment, secondary and tertiary grains grow.

Методом високочастотного (ВЧ) йонно-плазмового розпорошення в атмосфері аргону на монокристалічних підкладках NaCl та аморфних підкладках $\nu\text{-SiO}_2$ одержано тонкі плівки $(\text{La}_{0.06}\text{Ga}_{0.94})_2\text{O}_3:\text{Eu}$. Дослідження морфології поверхні тонких плівок методом атомно-силової мікроскопії показали, що з переходом від підкладок NaCl до $\nu\text{-SiO}_2$ зростає середній діаметер кристалітів, які формують плівку від 23 нм до 48 нм. Термооброблення плівок на підкладках з $\nu\text{-SiO}_2$ в атмосфері аргону приводить до зростання середніх діаметрів зерен до 68 нм і, відповідно, середньоквадратичної шерсткості від 0,5 нм до 6,1 нм. Проведено аналізу розподілів кристалітів за діаметром і за об'ємом та запропоновано, що у процесі ВЧ-напорошення відбувається зростання вторинних зерен, а у процесі високотемпературного термооброблення

відбувається зростання вторинних і третинних зерен.

Key words: gallium oxide, europium activator, thin films, crystallites, surface morphology.

Ключові слова: оксид Галію, європейовий активатор, тонкі плівки, кристаліти, морфологія поверхні.

(Received 28 July, 2023)

1. INTRODUCTION

Metal oxide materials play an important role among new functional materials for electronics. They are used in the creation of displays, scintillators, and means for recording and visualizing information. In this regard, pure and activated films based on $\beta\text{-Ga}_2\text{O}_3$ are widely used as thin-film materials, which are promising for field-effect transistors, luminescent displays, gas sensors, and UV-transparent electrodes [1–5]. In general, the optical and electrical characteristics of thin films based on $\beta\text{-Ga}_2\text{O}_3$ are determined by the methods of their preparation, deposition modes, substrate type, and processing technology as well as the introduction of impurities that can purposefully change the spectral-luminescent and electrophysical properties of these films. To this end, thin films with the chemical composition $(\text{La}_{0.06}\text{Ga}_{0.94})_2\text{O}_3:\text{Eu}$ were studied in this work, in which some Ga^{3+} ions were replaced by isovalent La^{3+} ions, that did not require local compensation of the electric charge. This substitution is because La_2O_3 films are also quite promising in terms of their use in optoelectronic and luminescent technology [6–8]. This also allows for a better study of luminescence centres in thin films based on $\beta\text{-Ga}_2\text{O}_3$, since the luminescence efficiency in these films is largely determined by the peculiarities of recombination processes, which are usually caused by luminescence centres of defective origin. The use of the Eu^{3+} ion as an activator is due to the fact that a number of films activated by this ion are quite promising red phosphors, which are widely used in optoelectronics [9–12].

In general, the question of the physical properties of thin films is complicated by the fact that films do not always have a perfect structure and can be polycrystalline, amorphous, or contain inclusions of other phases. Obtaining the required and stable reproducible properties of polycrystalline films is further complicated by the presence of intergranular boundaries (IGBs). The physical properties of polycrystalline thin films are largely determined not only by the material properties but also by the energy levels arising from the presence of the IGBs. It is clear that such levels are also determined

by the size of the crystallites, which form the thin films. This has led to the structural studies of $(\text{La}_{0.06}\text{Ga}_{0.94})_2\text{O}_3:\text{Eu}$ thin films reported in this paper. The films were obtained by the method of RF ion-plasma sputtering, which is optimal for obtaining homogeneous semiconductor and dielectric films [13].

2. EXPERIMENTAL TECHNIQUE

Thin films of $(\text{La}_{0.06}\text{Ga}_{0.94})_2\text{O}_3:\text{Eu}$ with a thickness of 0.2–1.0 μm were obtained by RF ion-plasma sputtering on single-crystal NaCl substrates and amorphous fused quartz $\nu\text{-SiO}_2$ substrates. The RF sputtering was carried out in an argon atmosphere in a system using the magnetic field of external solenoids for compression and additional ionization of the plasma column. After the films were deposited on $\nu\text{-SiO}_2$ substrates, they were heat treated in argon at 1000–1100°C. The starting materials were La_2O_3 , Ga_2O_3 , and Eu_2O_3 of the ‘oc. ч.’ grade. The concentration of the Eu^{3+} activator was 1 mol.%.

The structure and phase composition of the obtained films were studied by x-ray diffraction analysis (with Shimadzu XDR-600). The analysis of the diffractograms showed that the structure of these films corresponds to the monoclinic crystal structure of $\beta\text{-Ga}_2\text{O}_3$ and the results obtained are close to those obtained earlier for thin films of $\beta\text{-Ga}_2\text{O}_3$ and $(\text{Y}_{0.06}\text{Ga}_{0.94})_2\text{O}_3$ [14]. In particular, for polycrystalline $(\text{La}_{0.06}\text{Ga}_{0.94})_2\text{O}_3:\text{Eu}$ films, the predominant orientation of the films is observed in the (110), (002), (111), and (512) planes.

Using an OXFORD INCA Energy 350 energy dispersive spectrometer, elemental analysis of the samples was performed at several points on the surface of the films. The calculations confirmed that the percentage of components in the obtained films corresponded to their percentage in the compound $(\text{La}_{0.06}\text{Ga}_{0.94})_2\text{O}_3:\text{Eu}$.

The surface morphology of the films was studied using an INTEGRA TS-150 atomic force microscope (AFM).

3. RESULTS AND DISCUSSION

Microphotographs of the surface of $(\text{La}_{0.06}\text{Ga}_{0.94})_2\text{O}_3:\text{Eu}$ films obtained by RF ion-plasma sputtering on NaCl and $\nu\text{-SiO}_2$ substrates without heat treatment and after heat treatment in an argon atmosphere are shown in Fig. 1. The topography of the samples was quantitatively characterized by standard parameters: root-mean-square (RMS) roughness, maximum grain height, average grain diameter, average grain area, and grain volume, which were calculated from AFM data for areas of the same size (1000×1000 nm). The

characteristic parameters of $(\text{La}_{0.06}\text{Ga}_{0.94})_2\text{O}_3:\text{Eu}$ thin films on different substrates without heat treatment and after heat treatment in an argon atmosphere are given in Table 1. As can be seen from the results obtained, different types of substrates and the presence of heat treatment have a significant effect on the size of crystal grains and surface roughness of the films.

The analysis of AFM images (Fig. 1) and crystal grain parameters (Table) of the surface of $(\text{La}_{0.06}\text{Ga}_{0.94})_2\text{O}_3:\text{Eu}$ films shows that the films deposited on an amorphous substrate are formed from larger grains, than when sputtered on a single-crystal substrate with NaCl. Even larger crystallite sizes occur after heat treatment of the films. This increase in crystalline grain size and, in particular, the increase in the average grain diameter and RMS roughness indicate

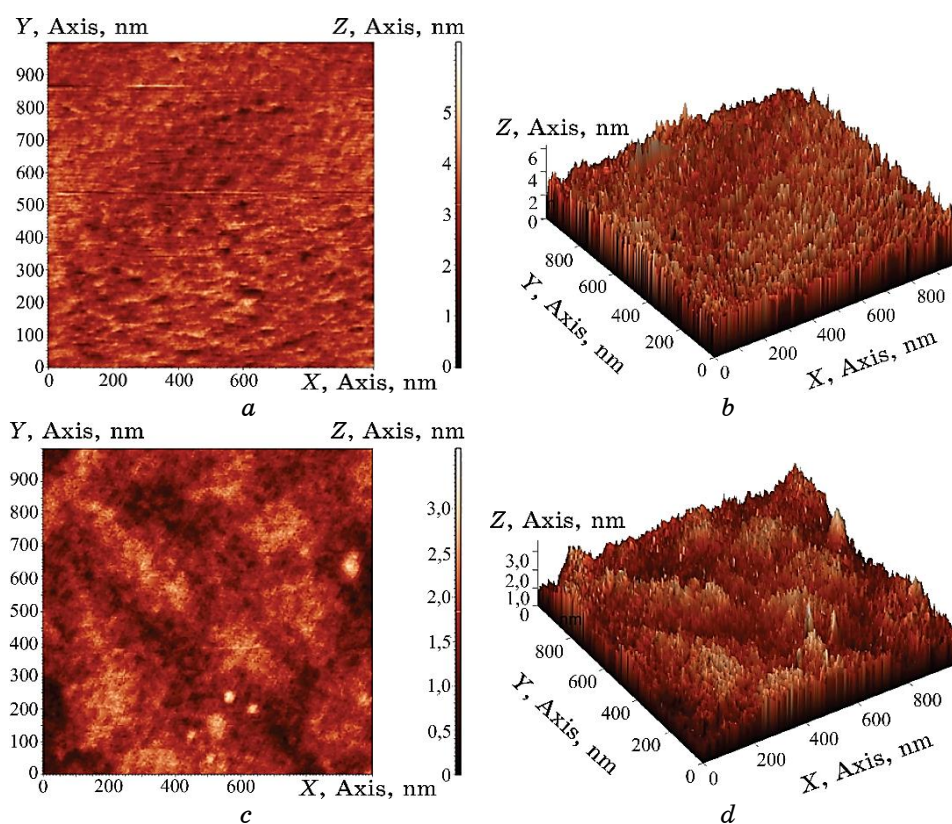
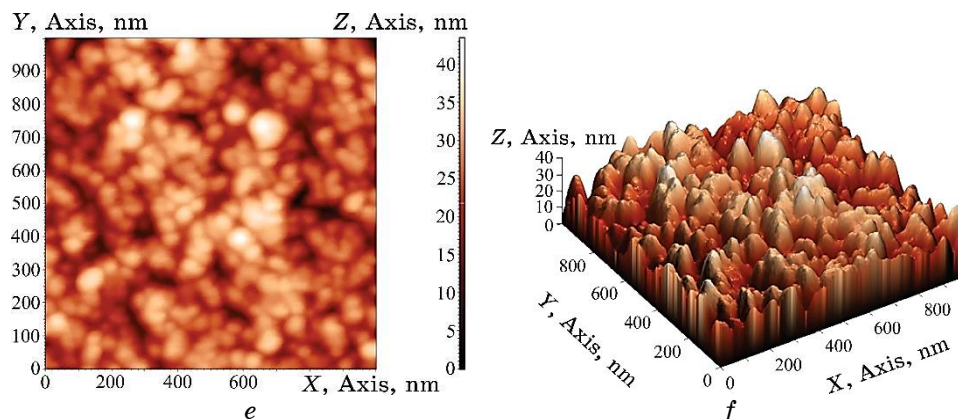


Fig. 1. Images of the surface morphology of $(\text{La}_{0.06}\text{Ga}_{0.94})_2\text{O}_3:\text{Eu}$ thin films obtained by RF sputtering without heat treatment on NaCl (*a, b*) and $v\text{-SiO}_2$ (*c, d*) substrates and after heat treatment in an argon atmosphere on $v\text{-SiO}_2$ substrates (*e, f*). Images *a, c* and *e* are two-dimensional, *b, d* and *f* are three-dimensional.



Continuation of Fig. 1.

TABLE. Crystalline grain parameters of thin films $(\text{La}_{0.06}\text{Ga}_{0.94})_2\text{O}_3:\text{Eu}$.

Parameter	No heat treatment on the NaCl substrate	No heat treatment on the $\nu\text{-SiO}_2$ substrate	Heat treatment in Ar on the $\nu\text{-SiO}_2$ substrate
Average grain diameter, nm	23	48	68
RMS roughness, nm	0.6	0.5	6.1
Maximum grain height, nm	3.3	2.1	17.9
Average grain area, nm^2	167	614	1516
Average grain volume, nm^3	56	145	4167

a more complex surface structure.

A comparison of the histograms of the grain-height distribution (Fig. 2) shows that taller grains are formed on the surface of $(\text{La}_{0.06}\text{Ga}_{0.94})_2\text{O}_3:\text{Eu}$ films on NaCl substrates, although their diameters are more than 2 times smaller. The high-temperature heat treatment of the films leads to a very significant increase in grain height. In particular, the root-mean-square roughness increases by more than 10 times.

The increase in the size of crystalline grains and the simultaneous decrease in the grain concentration in thin films of $(\text{La}_{0.06}\text{Ga}_{0.94})_2\text{O}_3:\text{Eu}$, when there is switching from NaCl to $\nu\text{-SiO}_2$ substrates, and, especially, the increase in the size of crystalline grains after heat treatment (Fig. 1) indicate the possibility of the

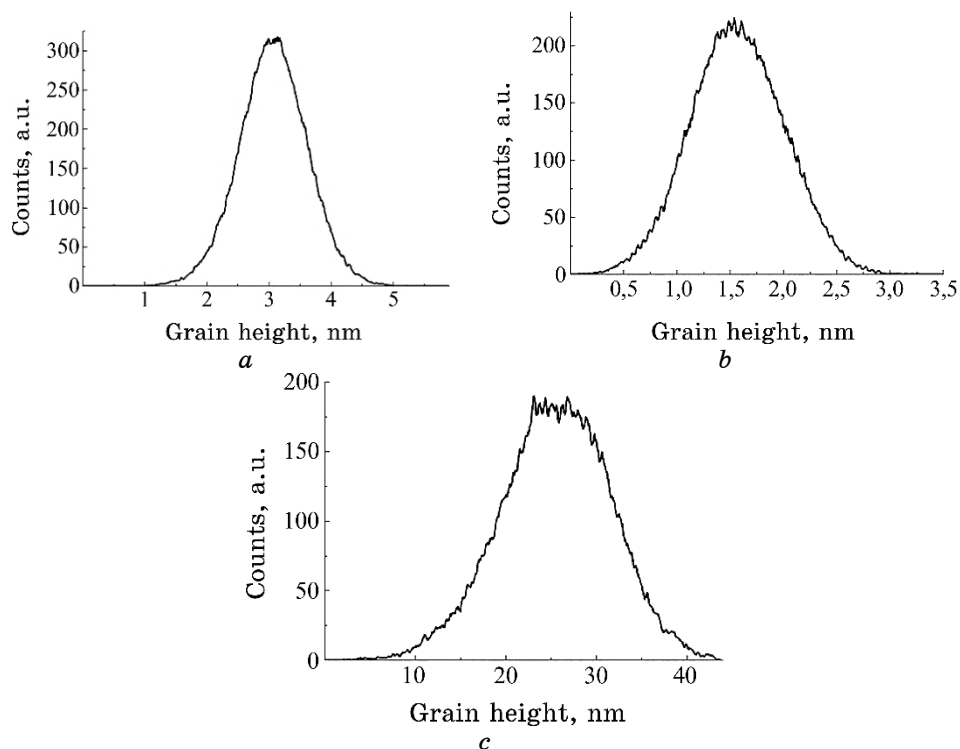


Fig. 2. Grain-height distribution on AFM images of $(\text{La}_{0.06}\text{Ga}_{0.94})_2\text{O}_3:\text{Eu}$ thin films obtained by RF sputtering without heat treatment on NaCl (a), $\nu\text{-SiO}_2$ (b) substrates and after heat treatment in argon on $\nu\text{-SiO}_2$ substrates (c).

transition of the film surface to a more nanostructured state due to the crystallization of the surface layer.

The characteristic distributions of grain diameter sizes in $(\text{La}_{0.06}\text{Ga}_{0.94})_2\text{O}_3:\text{Eu}$ thin films depending on the type of substrate and the presence of heat treatment are shown in Fig. 3.

A thorough review [15] analysed the growth of crystal grains in thin films and the evolution of crystal structures and showed that polycrystalline thin films with thicknesses up to 1 μm , which is typical for our $(\text{La}_{0.06}\text{Ga}_{0.94})_2\text{O}_3:\text{Eu}$ films, often have 2D-like structures. In such structures, most grain boundaries are perpendicular to the film surface. Most of the materials analysed in Ref. [15] form films from nonequilibrium grains with dimensions smaller than the film thickness and form two-dimensional structures only after annealing. Based on numerical results, it is also concluded in Ref. [15] that the formation of grains in thin films is difficult to describe accurately using modelling or comparison with experiments that

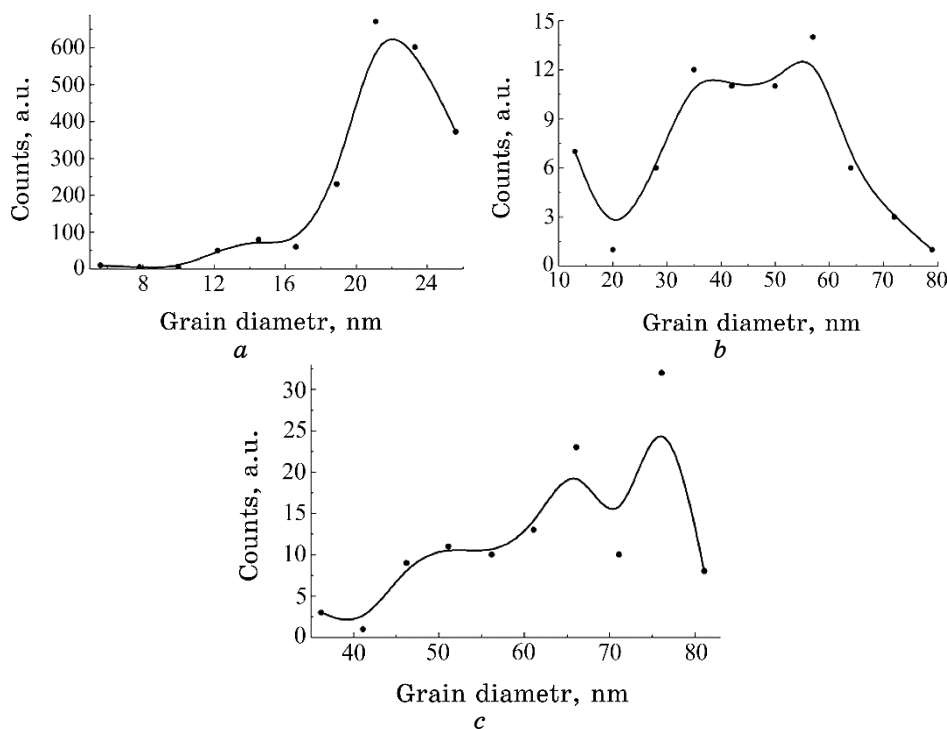


Fig. 3. Distribution of grain diameter sizes and calculated approximated diameter distribution on AFM images of $(\text{La}_{0.06}\text{Ga}_{0.94})_2\text{O}_3:\text{Eu}$ thin films without heat treatment on NaCl (a), $v\text{-SiO}_2$ (b) substrates and after argon heat treatment on $v\text{-SiO}_2$ (c) substrates.

described the study of foams or monolayers. In general, grain sizes in polycrystalline films are lognormally distributed in size.

In a number of cases, further grain growth is observed due to ‘anomalous’ growth or preferential growth of several grains, which usually have specific crystallographic orientation relations relative to the substrate surface plane. Our results show that this situation is most likely to be characteristic of the $(\text{La}_{0.06}\text{Ga}_{0.94})_2\text{O}_3:\text{Eu}$ films we obtained. When the number of growing grains leads to a ‘matrix’ of grains beyond the static boundaries, a bimodal grain size distribution develops, which is called secondary grain growth [16]. Grains that grow abnormally often have a limited or homogeneous texture. Secondary grain growth in thin films typically involves an evolution in the grain texture distribution as well as an evolution in the grain size distribution.

Our results of the distribution of grain diameter sizes in $(\text{La}_{0.06}\text{Ga}_{0.94})_2\text{O}_3:\text{Eu}$ thin films (Fig. 3) indicate that, when these films are deposited on NaCl substrates, an almost unimodal distri-

bution of diameters with a maximum in the 22 nm region is observed. A small local maximum in the region of 15 nm appears on the increasing part of the distribution. A more complex shape of the diameter distribution is formed, when the films are deposited on an amorphous ν -SiO₂ substrate. In particular, for freshly deposited films (Fig. 3, *b*), a bimodal distribution with maxima in the region of 37 nm and 57 nm is clearly visible. After heat treatment of such films, a trimodal distribution is already observed (Fig. 3, *c*) with maxima in the 52, 66, and 76 nm regions.

To summarise the situation described above, it can be concluded that secondary grain growth occurs during the RF spraying process. During heat treatment, secondary and tertiary grains grow. It should be noted that a similar situation is observed during RF deposition on ν -SiO₂ substrates and β -Ga₂O₃ thin films [17]. The growth of secondary and tertiary grains was observed in these films during both the RF sputtering and heat-treatment processes.

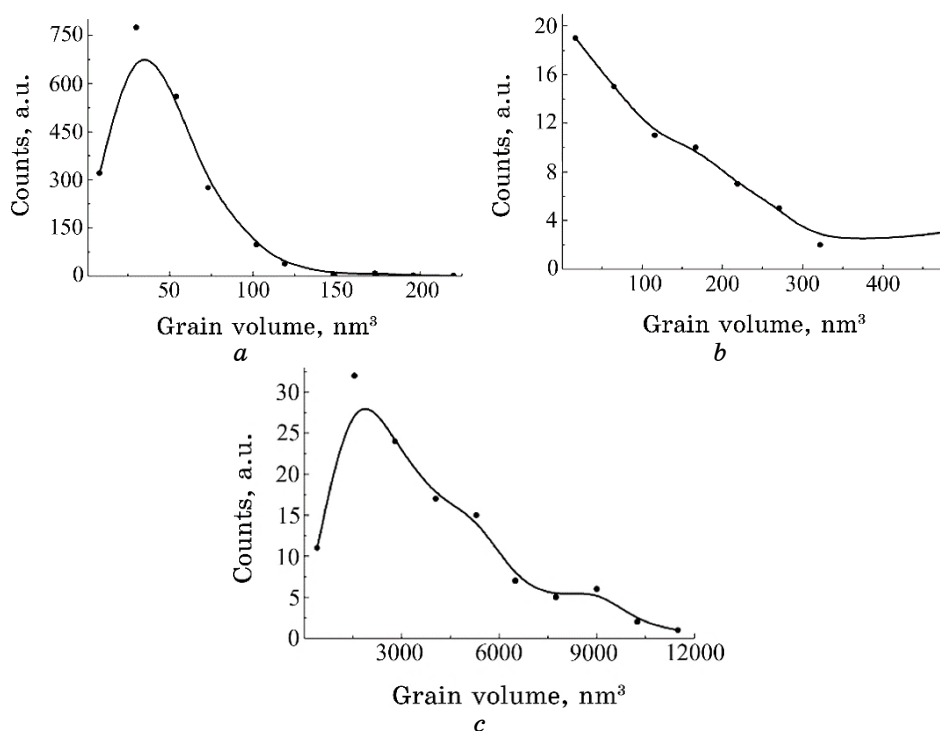


Fig. 4. Grain size distribution and calculated approximated volume distribution on AFM images of $(\text{La}_{0.06}\text{Ga}_{0.94})_2\text{O}_3:\text{Eu}$ thin films without heat treatment on NaCl (*a*), ν -SiO₂ substrates (*b*) and after argon heat treatment on ν -SiO₂ substrates (*c*).

Taking into account the presence of ‘anomalous’ grain growth and grain growth with specific crystallographic orientation relations relative to the substrate surface plane, we consider the distribution of grain volumes in $(\text{La}_{0.06}\text{Ga}_{0.94})_2\text{O}_3:\text{Eu}$ thin films.

As can be seen from Fig. 4, when thin films are deposited on a NaCl substrate, the distribution of grains by volume is quite well described by normal logarithmic law. This situation is typical for the distribution of grains by diameter in polycrystalline films [18]. In particular, this situation is observed during the RF deposition of $\text{Y}_2\text{O}_3:\text{Eu}$ thin films [19].

A similar situation is observed in thin films of $(\text{La}_{0.06}\text{Ga}_{0.94})_2\text{O}_3:\text{Eu}$ on $\nu\text{-SiO}_2$ substrates after heat treatment. At the same time, local maxima appear in the high-volume part of the distribution, which is most likely due to the growth of secondary and tertiary grains. For freshly deposited $(\text{La}_{0.06}\text{Ga}_{0.94})_2\text{O}_3:\text{Eu}$ films on $\nu\text{-SiO}_2$ substrates, a downward distribution is observed without local maxima that can be explained by the formation of nonequilibrium grains on the amorphous substrate.

To describe the obtained dependences (Fig. 4, *a* and *c*), we use the normal logarithmic law, which is used to describe the distribution of grains by diameter size in polycrystalline films [18] and which we will use to describe the distribution of grains by volume. By introducing the appropriate values, by analogy with Ref. [18], we obtain:

$$f(V) = \frac{1}{\sigma V \sqrt{2}} \exp \left[-\frac{(\ln V - \mu)^2}{2\sigma^2} \right],$$

where V is the grain diameter; $\ln(V - \mu)$ is the standard deviation (dispersion), and $\ln V$ is the average value.

The calculations show that, for the surface of $(\text{La}_{0.06}\text{Ga}_{0.94})_2\text{O}_3:\text{Eu}$ films, which are RF sputtered onto NaCl substrates, a lognormal distribution of grain volume with a maximum of about 35 nm^3 , and a dispersion of 0.35 is observed. When $(\text{La}_{0.06}\text{Ga}_{0.94})_2\text{O}_3:\text{Eu}$ films are deposited on $\nu\text{-SiO}_2$ substrates, a lognormal distribution of grain volume with a maximum of about 2000 nm^3 and a dispersion of 0.2 dominates.

4. CONCLUSIONS

It has been established that thin films of $(\text{La}_{0.06}\text{Ga}_{0.94})_2\text{O}_3:\text{Eu}$ formed from nanometre grains are formed by RF ion-plasma sputtering on single-crystal NaCl and amorphous $\nu\text{-SiO}_2$ substrates. Based on the AFM images, it is shown that the average diameters of the crystallites of the films on NaCl substrates are of 23 nm and on $\nu\text{-SiO}_2$

substrates are of 48 nm. The heat treatment of films on ν -SiO₂ substrates in an argon atmosphere leads to an increase in the average grain diameters to 68 nm and, accordingly, the root-mean-square roughness from 0.5 nm to 6.1 nm. Based on the analysis of the results of the distribution of grain diameter sizes, it is proposed that secondary grains grow in the process of RF sputtering. In the process of heat treatment, secondary and tertiary grains grow. At the same time, the grain volume distributions during the deposition of (La_{0.06}Ga_{0.94})₂O₃:Eu films on NaCl substrates and after heat treatment on ν -SiO₂ substrates correspond to a normal logarithmic distribution with one centre of a distribution.

REFERENCES

1. K. H. Choi and H. C. Kang, *Materials Letters*, **123**: 160 (2014); <https://doi.org/10.1016/j.matlet.2014.03.038>
2. Lingyi Kong, Jin Ma, Caina Luan, Wei Mi, and Yu Lv, *Thin Solid Films*, **520**, No. 13: 4270 (2012); <https://doi.org/10.1016/j.tsf.2012.02.027>
3. A. K. Saikumar, Sh. D. Nehate and K. B. Sundaram, *ECS J. of Solid State Science and Technol.*, **8**, No. 7: Q3064 (2019); <https://doi.org/10.1149/2.0141907jss>
4. M. Higashiwaki, *AAPPS Bulletin*, **32**: 3 (2022); <https://doi.org/10.1007/s43673-021-00033-0>
5. O. M. Bordun, B. O. Bordun, I. Yo. Kukharskyy and I. I. Medvid, *J. Appl. Spectrosc.*, **86**, No. 6: 1010 (2020); <https://doi.org/10.1007/s10812-020-00932-4>
6. C. V. Ramana, R. S. Vemuri, V. V. Kaichev, V. A. Kochubey, A. A. Saraev, and V. V. Atuchin, *ACS Appl. Mater. Interfaces*, **3**: 4370 (2011); <https://doi.org/10.1021/am201021m>
7. N. Pushpa, M. K. Kokila, and K. R. Nagabhushana, *Materials Letters: X*, **18**: 100205 (2023); <https://doi.org/10.1016/j.mlblux.2023.100205>
8. Kevil Shah, K. V. R. Murthy, and B. S. Chakrabarty, *Results in Optics*, **11**: 100413 (2023); <https://doi.org/10.1016/j.rio.2023.100413>
9. I. O. Bordun, O. M. Bordun, I. Yo. Kukharskyy, and Zh. Ya. Tsapovska, *Acta Physica Polonica A*, **133**, No. 4: 914 (2018); <https://doi.org/10.12693/APhysPolA.133.914>
10. J. Lakde, Ch. M. Mehare, K. K. Pandey, N. S. Dhoble, and S. J. Dhoble, *J. of Physics: Conference Series*, **1913**: 01229 (2021); <https://doi.org/10.1088/1742-6596/1913/1/012029>
11. Sh. Matsumoto, T. Watanabe, and A. Ito, *Sensors and Materials*, **34**, No. 2: 669 (2022); <https://doi.org/10.18494/SAM3698>
12. B. N. Rao, P. T. Rao, Sk. E. Basha, D. S. L. Prasanna, K. Samatha, and R. K. Ramachandra, *J. Mater. Sci.: Mater. Electron.*, **34**: 955 (2023); <https://doi.org/10.1007/s10854-023-10341-w>
13. K. Wasa, M. Kitabatake, and H. Adachi, *Thin Film Materials Technology: Sputtering of Compound Materials* (New York: William Andrew Inc. Publishing: 2004).
14. O. M. Bordun, B. O. Bordun, I. J. Kukharskyy, I. I. Medvid, O. Ya. Mylyo,

- M. V. Partyka, and D. S. Leonov, *Nanosistemi, Nanomateriali, Nanotehnologii*, **17**, Iss. 1: 123 (2019) (in Ukrainian); <https://doi.org/10.15407/nnn.17.01.123>
15. C. V. Thompson, *Sol. State Phys.*, **55**: 269 (2001); [https://doi.org/10.1016/S0081-1947\(01\)80006-0](https://doi.org/10.1016/S0081-1947(01)80006-0)
 16. C. V. Thompson, *J. Appl. Phys.*, **58**: 763 (1985); <https://doi.org/10.1063/1.336194>
 17. O. M. Bordun, B. O. Bordun, I. Yo. Kukharskyy, I. I. Medvid, I. I. Polovynko, Zh. Ya. Tsapovska, and D. S. Leonov, *Nanosistemi, Nanomateriali, Nanotehnologii*, **19**, Iss. 1: 159 (2021); <https://doi.org/10.15407/nnn.19.01.159>
 18. J. E. Palmer, C. V. Thompson, and Henry L. Smith, *J. Appl. Phys.*, **62**, No. 6: 2492 (1987); <http://dx.doi.org/10.1063/1.339460>
 19. O. M. Bordun, I. O. Bordun, I. M. Kofliuk, I. Yo. Kukharskyy, I. I. Medvid, Zh. Ya. Tsapovska, and D. S. Leonov, *Nanosistemi, Nanomateriali, Nanotehnologii*, **20**, Iss. 1: 91 (2022); <https://doi.org/10.15407/nnn.20.01.091>